Evaluation of NGMI in 128-Gbuad PAM4 O-Band 10-km Transmission Using MLSE Based on Nonlinear Channel Estimation and Decision Feedback

Shuto Yamamoto [(1)], Hiroki Taniguchi [(1)], Akira Masuda[(1)], Masanori Nakamura[(1)], Yoshiaki Kisaka[(1)]

[(1)] NTT Network Innovation Laboratories, NTT Corporation, shuto.yamamoto.at@hco.ntt.co.jp

Abstract *We demonstrate 128-Gbaud PAM4 transmission with 3-dB bandwidth of 20 GHz and show that advanced MLSE schemes achieve the higher performance not only in BER but also in NGMI. The NGMI deviates from the theoretical value because a simple method is utilized for LLR calculation. ©2022 The Author(s)*

Introduction

Recent increase of data-centre traffic due to the massive use of cloud services that handle rich content. A large number of connection ports are supported by Ethernet deployed economically and applied to intra- and inter-date centre networks. Ethernet has been already standardized up to 400GbE at 100-Gbps per channel with O-band and intensity-modulation and direct-detection (IM-DD) schemes in IEEE802.3 [1]. The next-generation Ethernet links such as 800GbE or 1.6TbE will require the increase of data rates even more. The higher modulation rate leads to bandwidth limitation (BWL) by transmission systems using narrowband and lower cost devices. BWL distorts the waveform of received signals as the inter-signal interference (ISI). To achieve high-capacity transmission economically, due to the nonlinear response caused by the drivers, modulators, and photo detectors, conventional linear equalization schemes are no longer able to cope with the severe nonlinear ISI. Against this, several studies about solving severe ISI with device nonlinearity in IM-DD systems are reported [2-8].

We have been focusing on the strong tolerance with maximum likelihood sequence estimation (MLSE) which is applied in a receiver-side digital signal processing (DSP) technique. We have proposed an advanced MLSE based on nonlinear-channel estimation and decision feedback (DF-NL-MLSE) for higher estimation accuracy of channel response and suppressing the amount of calculation of metrics in Viterbi algorithm (VA) [9]. In IEEE802.3, an application of soft-decision (SD) forward error correction (FEC) to high-baudrate IM-DD system is discussed [10, 11], and a performance evaluation for MLSE in SD-FEC scheme is required. In this paper, we demonstrate 128-Gbaud PAM4 O-band transmission with DF-NL-MLSE and show that DF-NL-MLSE achieves the higher normalized generalized mutual information (NGMI), which corresponds to the performance in SD-FEC scheme.

MLSE Based on Nonlinear Channel Estimation and Decision Feedback

A block diagram of DF-NL-MLSE is shown in Fig. 1. There are three adaptive filters which are a channel-shortening filter (CSF) and an adaptive low-pass filter (ALPF), and a desired impulse response filter (DIRF) [9]. The CSF compress the pulse width of received sequence. This shortens the response estimated by the DIRF and reduces the number of candidate sequences. In other words, the complexity of the calculation decreases exponentially. On the other hand, the CSF emphasizes high-frequency Gaussian noise. Therefore, the ALPF in the second stage suppresses it. Because the ALPF and the DIRF are updated on the basis of the same error function, the respective filters converge so that the Gaussian noise at the output of the ALPF becomes flat. In general, the inputs to the DIRF are generated as candidate sequences by VA. The VA is also responsible for managing information about state transitions and determines the symbols that represent the states that are traversed along the trellis path on the basis of the branch and path metrics. In this scheme, all sequence candidates are expanded to a Volterra series and input to the DIRF. It realizes that DIRF estimates nonlinear ISI without noise enhancement due to nonlinear calculation. Some decided symbols are then also input to the DIRF as a decision sequence to improve the estimation accuracy without long candidate sequences. The number of metric calculations is determined by the number of candidate sequences. So, this method of reducing the

$$f(\hat{d}_{-4}, \hat{d}_{-3}, c_{-2}, c_{-1}, c_0) = \sum_{a=-4}^{-3} p_a \hat{d}_a + \sum_{a=-2}^{0} q_a c_a + \sum_{a=-2}^{0} \sum_{b=-2}^{0} r_{ab} c_a c_b + \sum_{a=-2}^{0} \sum_{b=-2}^{0} \sum_{c=-2}^{0} s_{abc} c_a c_b c_c \, . \quad (1)$$

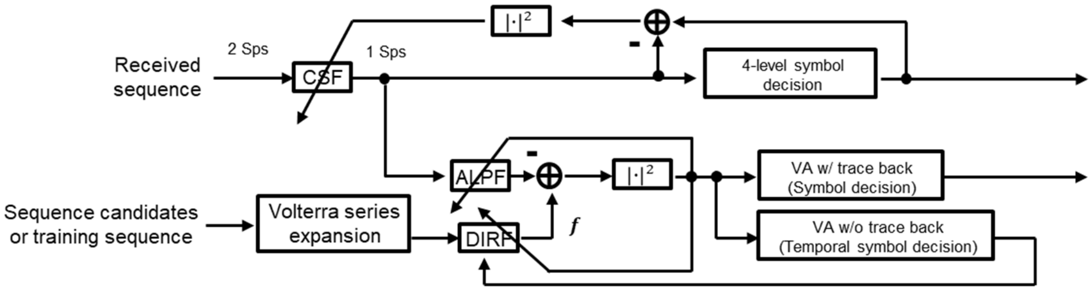

Fig. 1: Block diagram of DF-NL-MLSE.

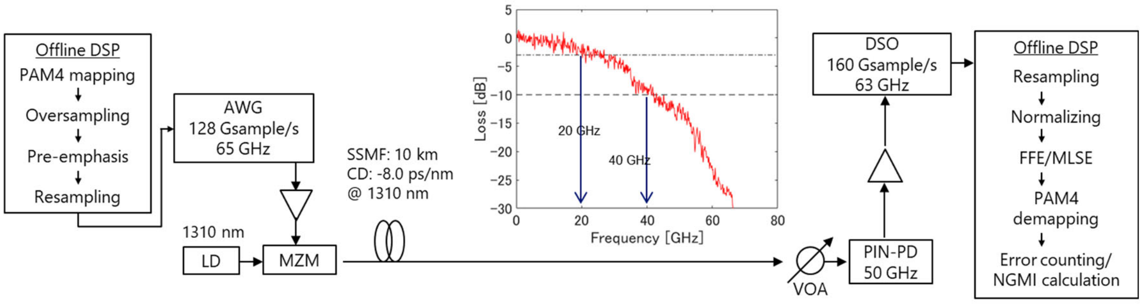

Fig. 2: Experimental configuration.

number of candidate sequences by shortening their length effectively reduces the complexity of the calculation. For example, if the length of the candidate sequence is three and the decision feedback is two symbols, the output f of the DIRF can be expressed as shown in Eq. (1). $\hat{d}_n$ is a decision feedback series from the Viterbi decoder. c_n is a selected sequence candidate. p_a, q_a, r_{ab}, and s_{abc} are taps and kernels. When updating the taps of the ALPF and the DIRF including the Volterra kernels, the training sequence or the decision sequence is input to the function of Volterra series expansion, and the difference between the outputs of the ALPF and the DIRF is used in a recursive least squares (RLS) algorithm.

Experimental Results

We demonstrate 128-Gbaud PAM4 10-km O-band transmission using DF-NL-MLSE and evaluate bit error ratio (BER) and NGMI. BER and NGMI correspond to the performances in hard-decision FEC (HD-FEC) and SD-FEC schemes, respectively. Figure 2 shows the experimental configuration. The transmission sequence is generated by an off-line DSP and a 65-GHz arbitrary waveform generator (AWG) driven at 1-sample/symbol. A 15th-order pseudo-random binary sequence is used as the prime of the transmission sequence. The electrical PAM4 signals are modulated to optical signals by a Mach-Zehnder modulator (MZM). The optical signals are transmitted to 10-km standard single-mode fibre (SSMF) without any optical amplifiers. Transmitted optical signals are received with a 50-GHz PIN photodiode (PD) after adjusting optical power by a variable optical attenuator (VOA). The amount of CD is –8.0 ps/nm in the case of 10-km transmission at 1310 nm. The received signals are then converted into a digital signal sequence by a 63-GHz, 160-Gsample/s digital storage oscilloscope (DSO) and demodulated by the conventional feed-forward equalizer (FFE) and the MLSE with or without nonlinear channel estimation and decision feedback. The finite impulse response (FIR) filter in the FFE and the CSF in the MLSE have 45 T/2-spaced taps. The number of T-spaced taps for the ALPF and symbols of candidate sequences are set to five. These filters are updated by the RLS algorithm. The order of Volterra series expansion is 3. The number of symbols with decision feedback is 20. To ensure the correct adaptation of the filters, the filter taps and kernels are pre-trained by the first 1000 symbols. Figure 2 also shows the frequency response of the transmission system, and it can be seen that the 10-dB bandwidth is 40 GHz, approximately. In contrast, the transmitted signal bandwidth is 64 GHz.

Figure 3 shows the relationship between received optical power (ROP) and BER or NGMI for the case with or without MLSE. NGMI is calculated based on bit logarithm likelihood ratio

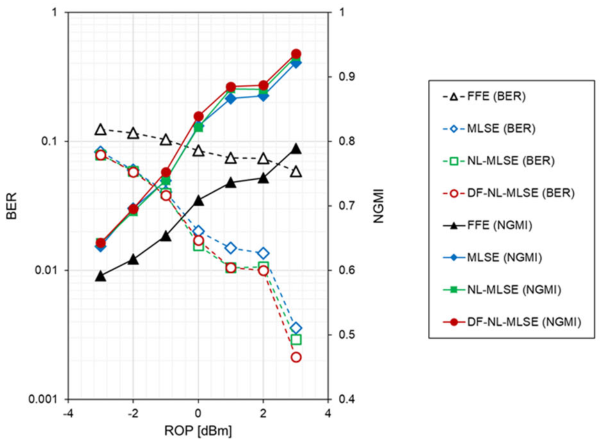

Fig. 3: Transmission performance with or without MLSE.

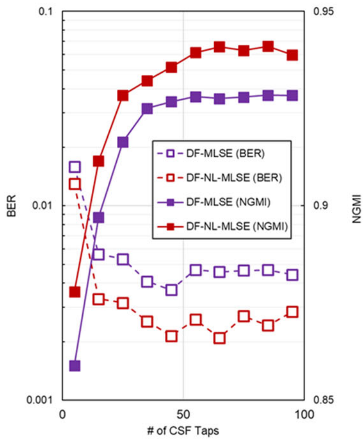

Fig. 4: Tap-length dependency.

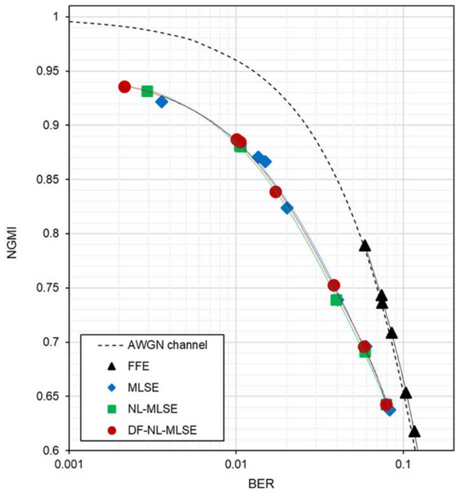

Fig. 5: Relationship between BER and NGMI.

(LLR) [12]. The LLR for the case with MLSE is calculated based on the minimum value of path metric for each bit composing PAM4 symbol in VA as shown in Eq. (2).

$$LLR \approx \frac{1}{2\sigma^2}\left(\min_{i\in U_0} l_i - \min_{i\in U_1} l_i\right), \qquad (2)$$

where l_i is i-th path metric in VA and $U_{0,1}$ is a set of indexes corresponding to bit 0 or 1. σ is a standard deviation of the noise distribution. This calculation method is very simple but a gain from trace back is not obtained in this method. As shown in Fig. 3, DF-NL-MLSE achieves the higher performance not only in BER but also in NGMI even if the simple method for LLR calculation is applied in the case with MLSE. This means that MLSE schemes including NL-MLSE and DF-NL-MLSE realize the higher performance not only for HD-FEC but also for SD-FEC. Figure 4 shows the relationship between the number of taps in CSF and BER or NGMI, in which the ROP is 4 dBm. As shown in this figure, the longer-tap CSF realizes the higher performance not only in BER but also in NGMI. Figure 5 shows the relationship between BER and NGMI. The dashed line is corresponding to the theoretical curve in additive white Gaussian noise (AWGN) channel. As shown in this figure, a conventional FFE scheme without MLSE achieves the performance same as that in the theoretical curve. On the other hand, the amount of NGMI in MLSE schemes is lower than that in the theoretical curve. This is because the simple method for LLR calculation applied in MLSE schemes does not include a gain from trace back in VA while the gain is obtained in hard decision which is utilized to calculate BER. This means that BER threshold for error-free operation is shifted in SD-FEC scheme with MLSE. We assume that the higher NGMI will be achieved for the case with MLSE if more complicated method which acquires the gain from trace back is applied.

Conclusions

We demonstrated 128-Gbaud PAM4 O-band 10-km transmission using MLSE based on nonlinear channel estimation and decision feedback in very severe bandwidth limitation with 10-dB bandwidth of about 40 GHz. We evaluated BER and NGMI for the case with or without MLSE and we showed that MLSE schemes including NL-MLSE and DF-NL-MLSE achieved the lower BER and higher NGMI. This means that MLSE realizes the higher performance not only for HD-FEC but also for SD-FEC. In this evaluation, a simple method was utilized in order to calculate a bit LLR in which the LLR was calculated based on the minimum value of path metric for each bit composing PAM4 symbol in Viterbi algorithm. We also showed the relationship between BER and NGMI. The NGMI for the case with MLSE is lower than the theoretical curve because a gain from trace back is not obtained in the simple method for LLR calculation.

References

[1] IEEE 802.3cu-2021 - IEEE Standard for Ethernet - Amendment 11: Physical Layers and Management Parameters for 100 Gb/s and 400 Gb/s Operation over Single-Mode Fiber at 100 Gb/s per Wavelength

[2] N. Stojanovic et al., "210/225 Gbit/s PAM-6 Transmission with BER Below KP4-FEC/EFEC and at Least 14 dB Link Budget," in Proc. ECOC, We1H.5, 2018.

[3] X. Chen et al., “Single-wavelength and single-photodiode 700 Gb/s entropy-loaded PS-256-QAM and 200-GBaud PS-PAM-16 transmission over 10-km SMF”, in Proc. ECOC, Th3A-2, 2020.

[4] Q. Hu et al., “120 Gbaud IM/DD PAM4-transission over 1.5 km SMF Using a single CMOS DACwith < 20 GHz analog bandwidth”, in Proc. ECOC, Tu1E-5, 2020.

[5] K. Schuh et al., "High-speed IM/DD transmission with analog (de-)multiplexers," in Proc. ECOC, We1C1.1, 2021.

[6] M. S. Bin Hossain et al., "402 Gb/s PAM-8 IM/DD O-band EML transmission," in Proc. ECOC, We1C1.4, 2021.

[7] N. Kikuchi et al., "Application of generalized THP for arbitrary PAM level design in short-reach IM/DD signaling," in Proc. ECOC, We3C2.6, 2021.

[8] J. Cho et al., “Volterra equalization to compensate for transceiver nonlinearity: performance and pitfalls,” in Proc. OFC, W2A.36, 2022

[9] H. Taniguchi et al., "800-Gbps PAM-4 O-band transmission through 2-km SMF using 4λ LAN-WDM TOSA with MLSE based on nonlinear channel estimation and decision feedback," in Proc. ECOC, We1C1.3, 2021.

[10] https://www.ieee802.org/3/df/public/22_02/lu_3df_01b_220215.pdf

[11] https://www.ieee802.org/3/df/public/22_02/wang_3df_01_220215.pdf

[12] A. Alvarado et al., “Replacing the soft-decision FEC limit paradigm in the design of optical communication systems”, Journal of Lightwave Technology, vol. 33, no. 20, pp. 4338–2352, 2015.